doi:10.1017/S1431927618012679
Microsc. Microanal. 24 (Suppl 2), 2018


# Numerical Analysis of Antiphase Domain Boundaries in a FeAl Alloy Using X-Ray Bragg Coherent Diffractive Imaging

Chan Kim[1,*], Virginie Chamard[2], Jörg Hallmann[1], Wei Lu[1], Ulrike Boesenberg[1], and Anders Madsen[1,**]

[1] European XFEL GmbH, Holzkoppel 4, 22869 Schenefeld, Germany
[2] Aix-Marseille University, CNRS, Centrale Marseille, Institut Fresnel, Marseille 13013, France
[*] Corresponding author, chan.kim@xfel.eu
[**] Corresponding author, anders.madsen@xfel.eu

Phase retrieval is one of the most critical steps in coherent X-ray diffractive imaging (CDI) [1-3], specifically in the Bragg scattering geometry, where crystalline distortions such as strain, tilt, or anti-phase domain (APD) introduce strong fluctuations in the phase of the effective complex value electron density [4,5]. The retrieved sample image corresponds to the convolution of the true effective electron density with the resolution function of the experiment. However, the currently best available image resolution (smallest pixel/voxel) with CDI is limited to the nanometer range [6,7], mostly due to experimental limitations such as limited X-ray photon flux or set-up instability, while crystalline distortion variations are often of smaller extent and corresponds to large phase shift. This convolution results in a degraded image, where the modulus of the effective electron density function, which is related to the sample electron density, cannot be reliably obtained [8]. In this paper we show that the image distortion problem can be minimized if we employ a modulus homogenization (MH) constraint [9]. We demonstrate how the convolution effect leads to an incorrectly retrieved modulus in regular CDI and show the efficiency of the MH constraint in obtaining a reliable APD reconstruction.

As a sample specimen we modeled a 2D Fe-Al alloy crystal in the B2 phase [10], containing two APDs separated by an anti-phase domain boundary (ADB) that is formed due to the degeneracy in ordering of atoms on the sub-lattice. Here a real atomistic model with exact number of electrons in each atomic position was used. In this case it results in a $\pi$ phase shift of the (01) and (10) superlattice Bragg peaks. In addition, we applied lattice displacement to the model yielding a phase shift of 0.3 rad for the (01) superlattice reflection and 0.6 rad for the (02) fundamental reflection. The calculated diffraction intensity in reciprocal space and modulus of the corresponding real space electron density of the crystal are illustrated in Fig. 1(a) and (b), respectively. The line near the middle of the crystal seen in Fig. 1(b) corresponds to an ADB where two iron atoms are nearest neighbors. The effect of the ADB is clearly visible in coherent scattering pattern giving rise to divided central speckles in the (01) and (10) peaks (Fig. 1(a)).

Phase retrieval employing a guided hybrid input-output (GHIO) algorithm [11] was applied to the (00), (01), and (02) Bragg peaks, corresponding to limited views of the reciprocal space. The results are shown in Fig. 1(c-j). The reconstructed phase of the (00) peak (Fig. 1(c)), of which diffraction pattern is recorded in transmission geometry, shows no displacement and APD effects. The displacement and APD are visible from the reconstructed phases of the (02) and (01) peaks (Fig. 1(d) and (e)) but the value of the phase is not correct, particularly for the (01) reconstruction. The larger a phase step, the worse the reconstructed phase map becomes. This can also be observed by investigating the reconstructed moduli (Fig. 1(g-i)). With a strong phase shift, such as an APD, in the scattering volume, the retrieved amplitude strongly fluctuates and even decreases down to zero, particularly in the (01) reconstruction where the APD phase sensitivity is high. If the retrieved amplitude is close to zero, the

phase retrieval algorithm can put any phase value into that pixel and consequently the whole reconstruction is affected (Fig. 1(e) and (i)).

To compensate the convolution (averaging) effect in the Bragg reconstruction, we employed the MH constraint and applied it to the (01) reconstruction. The quality of the retrieved modulus, Fig. 1(j), improves (no zero density region) and becomes smooth although there still exists a weak averaging effect near the ADBs. The retrieved phase, Fig. 1(f), becomes sharper and better especially near the ADB where the correct value of the phase shift ($\pi$) now is found. To conclude, averaging cannot be totally avoided in phase retrieval processes until a true atomic resolution CDI method is found, but the MH constraint can minimize this effect and dramatically improve image reconstructions in materials science, as demonstrated here for APDs in crystals.

References:

[1] H. N. Chapman and K. A. Nugent, Nat. Photonics **4** (2010), p. 833.
[2] J. Miao *et al*, Nature **400** (1999), p. 342.
[3] M. A. Pfeifer *et al*, Nature **442** (2006), p. 63.
[4] F. Mastropietro *et al*, Nat. Mater. **16** (2017), p. 946.
[5] W. Cha *et al*, Nat. Mater. **12** (2013), p. 729.
[6] D. A. Shapiro *et al*, Nat. Photonics **8** (2014), p. 765.
[7] Y. Takahashi *et al*, Phys. Rev. B **80** (2009), p. 054103.
[8] P. Godard *et al*, Opt. Express **20** (2012), p. 25914.
[9] P. Godard *et al*, Phys. Rev. B **84** (2011), p. 144109.
[10] L.-M. Stadler *et al*, Phys. Rev. B **69** (2004), p. 224301.
[11] C.-C. Chen *et al*, Phys. Rev. B **76** (2007), p. 064113.

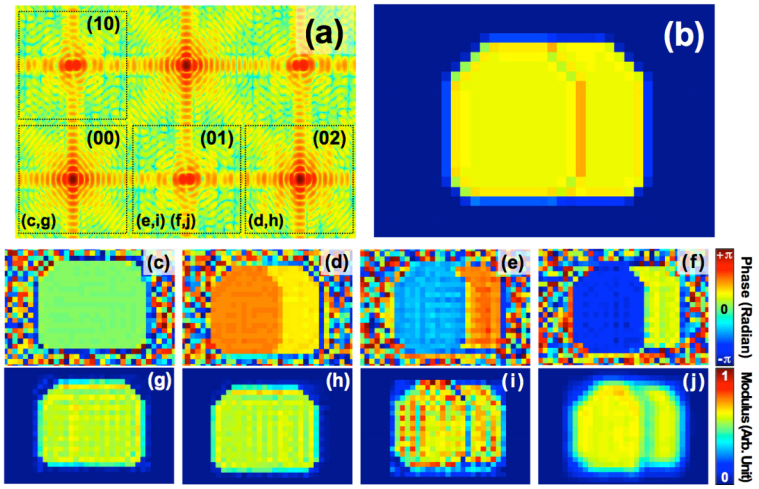


**Figure. 1.** (a) Calculated diffraction intensity from a B2 structured Fe-Al alloy model crystal which contains an APD ($\pi$ phase shift only at (01) and (10) reflections) together with lattice displacement (0.3 rad for (01) and 0.6 rad for (02) reflections) at the domain boundary. (b) Real space modulus, which is proportional to the electron density. The orange line near the middle of the crystal corresponds to the ADB. (c-j) Reconstructed phases (upper row; c-f) and moduli (bottom row; g-j) by guided hybrid input-output (GHIO) algorithm at (c,g) (00) peak, (d,h) (02) peak, and (e,i) (f,j) (01) peak. The MH constraint was only applied to the (f,j) reconstruction.

https://doi.org/10.1017/S1431927618012679 Published online by Cambridge University Press